

Structural Comparison of Premotor Neurons in Silkworm Moths

Kanako Nakajima^{1*}, Soichiro Morishita², Hajime Asama², Tomoki Kazawa³, Ryohei Kanzaki³ and Taketoshi Mishima⁴

¹Fujita Corporation, 4-25-2 Sendagaya, Shibuya-ku, Tokyo 151-8570, Japan

²RACE, The University of Tokyo, 5-1-5 Kashiwanoha, Kashiwa, Chiba 277-8568, Japan

³RCAST, The University of Tokyo, 4-6-1 Komaba, Meguro-ku, Tokyo 153-8904, Japan

⁴Saitama University, 255 Shimo-okubo, Sakura, Saitama, Saitama 338-8570, Japan

*E-mail address: kanako.nakajima@fujita.co.jp

(Received July 25, 2009; Accepted September 12, 2009)

In most cases, differences in neuronal function depend on the neuronal structure, and it is thought that shape and structure are closely connected. However, a relationship between neuronal shape and function is not elucidated because there are no elucidation methods beyond a visual comparison. This paper objectively compares the neuronal structure with several structural features which are extracted from the three-dimensional form of a silkworm moth's neuron. These features are based on biologist's knowledge in morphology of a silkworm moth's neuron; a second-order moment represents the positional relation of nerve fibers, and eigenvalues of variance-covariance matrix of coordinate values of nerve fibers represent a spatial extent of nerve fibers. In the result, objectively structural dissimilarity and similarity between neurons are found; ambiguous evaluation criterions of biologists are quantified. In addition, structural features which are strongly associated with the function of premotor neurons are found.

Key words: Objective Comparison, Structural Analysis, Three-Dimensional Form, Premotor Neuron

1. Introduction

Animate beings have been gaining structures and functions of the brain throughout evolutionary history. In particular, adaptation to environmental changes is essential for surviving. Insects are flexibly adaptive to environmental changes (Karl, 1974; Ikeno, 2004; Kawabata *et al.*, 2007), but they have far simpler and smaller nervous systems than mammals do. Consequently, insects are particularly useful in research for analyzing and understanding the basic principles of nervous information propagation.

Because nervous information in the brain is propagated by binding to neurons, this specific neuronal function is reflected in the large diversity of dendritic morphologies of neurons; differences in morphologies between neurons are closely related to their function. For this reason, elucidating the mechanisms by which different neuron class-specific morphologies are defined is important for understanding of neuronal function. Therefore, research into structure of neurons in insect brains has been emphasized to analyze neural networks and mechanisms of information propagation in the brain (Kanzaki *et al.*, 1994; Jaap *et al.*, 2001; Yamanaka *et al.*, 2005; Ridgel *et al.*, 2007; Nishikawa *et al.*, 2008).

Single neurons of a silkworm moth have been analyzed in order to elucidate the mechanisms of information propagation. As a result of their analysis, three neurons which control pheromone behavior have been found, and physiological response characteristics and a difference of shape are well investigated. These characteristics of physiological response and neuronal shape classify three neurons as two categories, respectively. However, categorized results using physiological response characteristics and cat-

egorized results using shape characteristics are different. Three neurons (neuron1, neuron2, and neuron3) are classified as {neuron1, neuron2 and neuron3} using physiological response characteristics and as {neuron1 and neuron3, neuron2} using shape characteristics. Therefore the relationship between neuronal function and shape is not clear.

Then we employ neuronal structure as an indicator of elucidation of the relationship between neuronal function and shape. It is thought that if neurons have similar shape characteristics, they have similar structures. In addition, it is thought that if neurons have similar structures, these neurons have the similar function. When this two assumptions are truth, it turn out that neurons which have similar shape characteristics have the similar function. However there is a discrepancy between categorized results and above assumptions because results using physiological response characteristics and using shape characteristics are different as previously indicated. This means either or both assumptions are false. Previously, neuronal shapes are observed visually. For this reason, the detail of shape characteristics is not clear. Additionally, it is not necessary true that neurons which have similar shapes have similar structure. Moreover, though there are individual differences in the same neuron's shape, these neurons have same function. However structural and shape features which are strongly associated with neuronal function are not clear. It is thought that objective comparison of neuronal structure makes these relationships clear.

In this paper, we accept the assumption that neurons have same structures have the same function. We compare structures of behaviorally relevant neurons of silkworm moths objectively. This paper examines the objective comparison

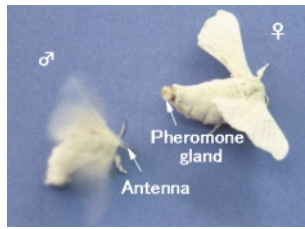


Fig. 1. Male silkmoth moth and female silkmoth moth.

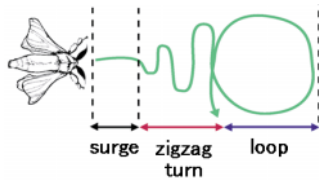


Fig. 2. Sex pheromone-searching behavior of male silkmoth moth.

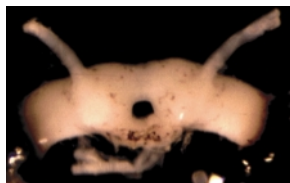


Fig. 3. Silkmoth moth brain.

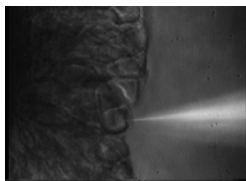


Fig. 4. Injection of a fluorescent dye into a single neuron.

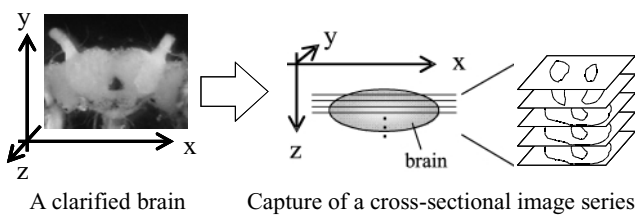


Fig. 5. Capture of the cross-sectional image series by CLSM.

of neuronal structure using image processing techniques and statistics which are extracted from images of a neuronal three-dimensional form.

2. Adaptive Behaviour of a Silkmoth Moth and Neurons

2.1 Pheromone-searching behavior and premotor neurons

An instinctive behavior of insects is one that is essential to their survival and it is thought that the instinctive behavior is an innate behavior which has been refined in process of the evolution of insects. A typical instinctive behavior is

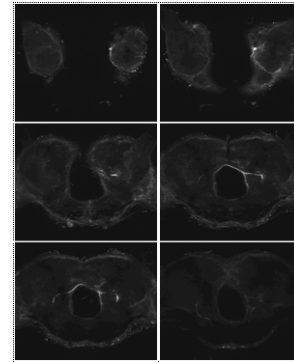


Fig. 6. Example of a cross-sectional image series with CLSM.

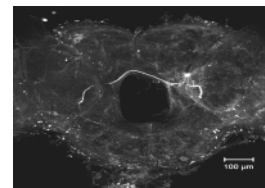


Fig. 7. Projection image of the cross-sectional image series with CLSM.

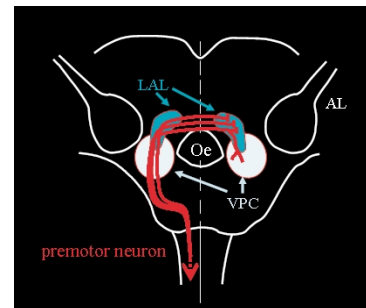


Fig. 8. Simplified schematic of a silkmoth moth brain and premotor neurons (AL: Antenna Lobe).

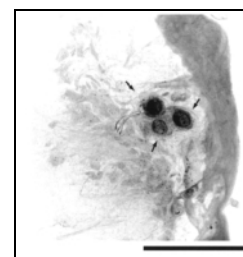


Fig. 9. Soma of premotor neuron (scale bar = 100 μm).

the sex-pheromone search behavior of the male silkmoth moth: *Bombyx mori*. The male silkmoth moth behaves in this way only when his antenna receives sex pheromone of female silkmoth moth as shown Fig. 1. This instinctive behavior comprises a well defined series of behaviors: pheromone reception is followed by a surge, a zigzag turn, and a loop (Fig. 2). This sequence can be initialized by an additional pheromone reception (Kanzaki *et al.*, 1992). Therefore, trajectories of silkmoth moth's locomotion are changeable by pheromone stimuli level such as pheromone

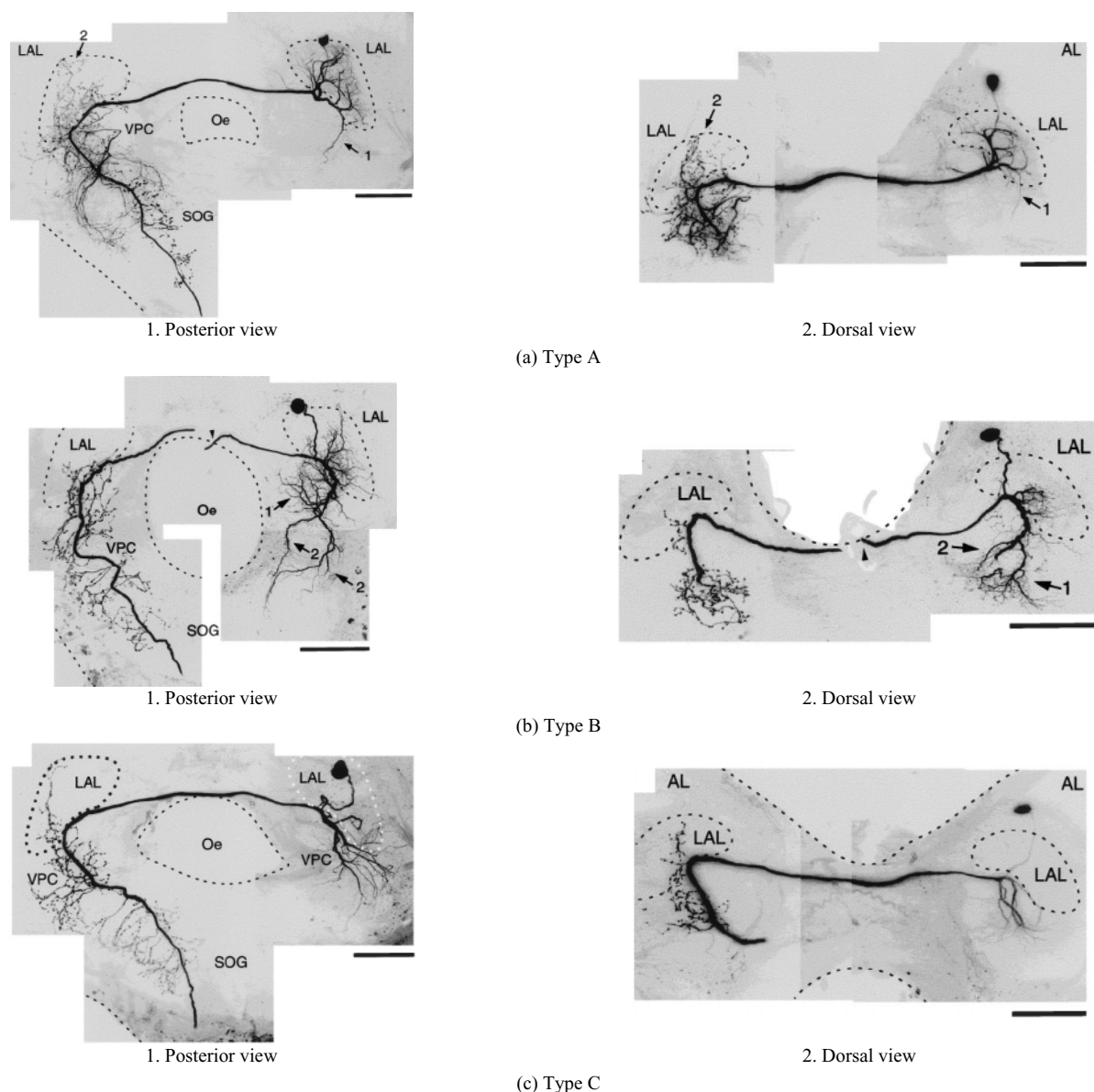


Fig. 10. Projection image of premotor neuron (excepted from Mishima and Kanzaki (1999)).

concentration.

One of elements generating this pheromone behavior is the premotor neuron and it was reported that these neurons are divided into two types in the silkmoth brain: G-1 and G-2 (Mishima and Kanzaki, 1999; Wada and Kanzaki, 2005). There are only three premotor neurons (G-1) and these neurons have been identified. In addition, the timing for shifting the turning direction of the silkmoth moth is synchronized to the sideways head movements and premotor neurons (G-1) relate to control of this synchronization. Therefore, structural analysis of premotor neurons (G-1) is important to elucidate pheromone behavior mechanisms in the silkmoth moth. By contrast, there are about fifteen premotor neurons (G-2) some of which have not been identified yet. For these reason, first of all, this paper covers premotor neuron (G-1).

2.2 Structure and function of premotor neurons

In essence a neuron that receives input expresses action potential, and propagates information to other neurons.

This information is modified by receiving input from several neurons and changing a threshold of expression of action potential. This means expression of neuronal function depends on structure of it. Therefore it is thought that if neurons have the similar structure, these neurons will express similar function.

A single neuron's form is needed for structural analysis of the neuron for elucidation of neuronal function. In this paper, *form* is used to describe morphology and topological characteristics of a neuron, *shape* is global shape and appearance, and *structure* describes more detailed characteristics than *shape*: local shape, the number of dendrites, and location of dendrites. Form and physiological response characteristics of premotor neurons has been observed.

2.2.1 Observation of a premotor neuron's form
Seki *et al.* (2005) proposed a method for observation of a single neuron three-dimensionally using confocal laser scanning microscopy (CLSM). A single neuron is observed three-dimensionally by the following steps.

Table 1. Physiological response characteristics of premotor neurons (excepted from Mishima and Kanzaki (1999)).

Response	Type of neuron		
	Type A	Type B	Type C
Flip-Flop	3	0	0
Long-lasting inhibition	0	3	2
No response	0	1	0
Total	3	4	2

1. Impale an intended single neuron on a glass micro-electrode filled with a fluorescent dye.
2. Apply a 1–10 nA electrical current to a glass electrode for injection of the dye into the neuron.
3. Fix the brain in formaldehyde, dehydrate it using an ethanol series, and clarify it using methyl salicylate to obtain high-S/N samples.
4. Capture the cross-sectional image series of a single neuron using confocal laser scanning microscopy (CLSM).
5. The cross-sectional image series are reconstructed as three-dimensional data: voxel data.

In the steps described above, because the central axis of images is not out of alignment, it is possible to capture high-quality images. Figure 3 shows the silkworm moth brain and Fig. 4 also shows the appearance of injection of a fluorescent dye into a single neuron in the silkworm moth brain. Figure 5 illustrates a schematic diagram of capturing an image series with CLSM; Fig. 6 shows an example of a cross-sectional image series obtained using CLSM. Figure 7 presents a projection image of the cross-sectional image series.

2.2.2 Shape and structural characteristics and physiological response of premotor neurons Figure 8 shows a simplified schematic of a silkworm moth brain. A silkworm moth has two LAL (lateral accessory lobes) and two VPC (ventral protocerebrum) in the brain as shown Fig. 8. Figure 9 shows the somas of three premotor neurons.

These neurons are closely-situated and lie astride LAL and VPC which are located on both sides of the brain. Mishima and Kanzaki (1999) have categorized premotor neurons into three types (i.e., Type A, B, and C) based on detailed morphological observations as pictured in Fig. 10. In morphological characterization of premotor neurons by visual observation, they focus attention on neuronal arborization in LAL which is ipsilateral to the soma as indicated Figs. 10-(a)2, -(b)2, and -(c)2. As the result, they were characterized as below.

[Type A]

Neuronal arborizations spread extensively in almost the whole LAL (Fig. 10-(a)2). Additionally, the way the main branch which is the longest and thickest neurite extends is different from the other Type and one small neurite extends to the VPC (Fig. 10, arrow 1).

[Type B]

Fine dendrites are into the medial part of the LAL. These dendrites in the LAL appear to be less extensive than dendrites from Type A (Fig. 10-(b)2). In addition, some neuronal arborizations extend to the VPC (Fig. 10-(b)1, arrow

1 and 2).

[Type C]

No processes are observed in the LAL (Fig. 10-(c)2) but neuronal arborizations extend to the VPC (Fig. 10-(c)1).

In addition, Table 1 shows results of electrophysiological response of premotor neurons (Mishima and Kanzaki, 1999). In these result, Type A of premotor neuron shows a “Flip-Flop” response and Type B and Type C show a “Long-lasting inhibition” response. This means silkworm moth has redundancy of function in the brain; three premotor neurons include spare a neuron.

This spare neuron allows normal propagation even if one of them breaks.

2.3 Issue in structural and functional elucidation of premotor neurons

As previously indicated, neuronal structure and function are closely connected. In addition, it is thought that neuronal shape and structure also are closely connected. With these relations, it is thought that neuronal shape and function are closely connected; neurons which have same shape characteristics have the same function. However, in previous research, there is difference of opinion about category of premotor neurons. Mishima and Kanzaki (1999) guesses that premotor neurons are classified three types based on shape characteristics and structure by appearance, physiological response results of them. On the other hand, one guesses these neurons are classified two types based on shape characteristics of them by appearance; Type A is similar to Type C in visual, though physiological responses of Type A and Type C are different.

It is thought that the above difference of opinion occurs through visual comparison; visual comparison lacks credibility because it depends on an observer. We cannot categorically state that premotor neurons have three or two types though there are no further methods of analysis biologically except for visual comparison or using physiological response characteristic. Because it is thought that two neurons have similar physiological response in the case that the structure of neuron is similar even if the shape is different.

In addition, the relationship between neuronal shape and structure is not clear. Moreover, differences and structural similarities between three premotor neurons or individual are not shown in detail. Even if shape is different, naturally it is possible to have the similar function, but the characteristic of the shape and structure that are strongly associated with neuronal function are not clear.

If the relationship between neuronal shape and structure is clear, it is thought that the relationship between neuronal shape and function is demonstrable. Analyzing in more detail of three premotor neurons, these relationships become apparent.

Then this paper compared structure of neurons in more detail and objectively by using image processing techniques.

2.3.1 Structural comparison of neurons In some previous works on structural comparison of neurons, several methods are reported. For example, Sandeep *et al.* (2008) presented difference in structure using gray values of a two-dimensional projection image of a fluorescently-

Table 2. Feature for structural comparison.

Feature	Amount of characteristics	Point of a biologist's observation
1	A ratio of right side in whole main branch's length	Key point 1
2	Correlation coefficient of curvature and length of the main branch	Key point 1
3-1	Average of distance from the origin to each branching point on the main branch	Key point 2
3-2	Second-order moment of distance from the origin to each branching point on the main branch	Key point 2
4	Coordinate value's variation of sub-branch which are in the near origin	Key point 2
5-1	Average of angles between the main branch and sub-branch	Key point 3
5-2	Variation of angles between the main branch and sub-branch	Key point 3

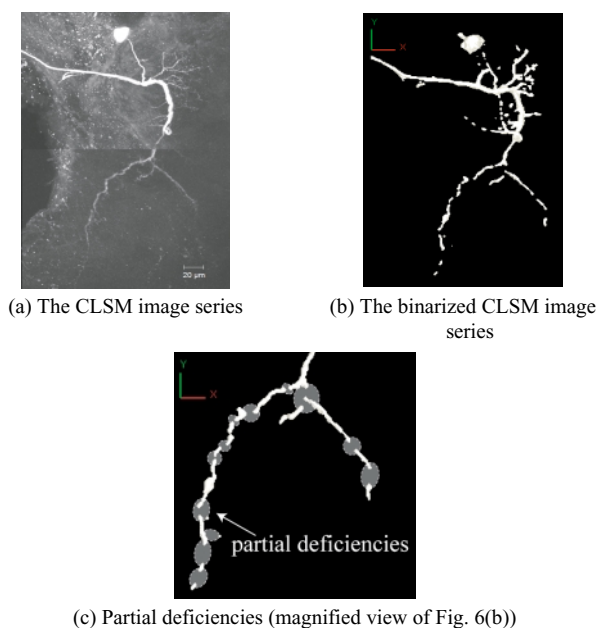


Fig. 11. Example of partial deficiencies through the threshold process (a projection image).

stained neuron, and Evers *et al.* (2006) analyzed visually by using a dendritic graph expression. However, these structural features depend on the subjective decision of an observer or experimental conditions. In addition, a dendritic graph needs laborious work.

On the other hand, Urata *et al.* (2007) proposed a method for automatic three-dimensional classification of silkworm moth's neuron types which is not a premotor neuron using features which are extracted from CLSM image series. This feature which used by Urata *et al.* (2007) indicates whole structure of neurons and means a complexity measure of structure.

However, because characteristics in the form of a premotor neuron are not seen only globally but also locally, the amount of characteristics which had been proposed by previous works is just a few of the characteristics. Then we need to employ a new amount of characteristics for structural comparison between premotor neurons.

3. Proposed Method

3.1 Extraction of a single neuron's form

The three-dimensional form of a single neuron is necessary to analyze the structures of the neuron. Gener-

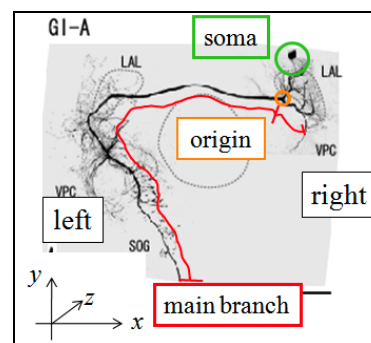


Fig. 12. Definitional word.

ally, this model is reconstructed with a single neuron's cross-sectional image series which is obtained by extracting regions of a fluorescently stained neuron from the image series captured using CLSM. In this paper, the three-dimensional form of a single neuron is extracted automatically using the method which we have proposed (Nakajima *et al.*, 2009). During the threshold process which is one of a region extraction process which is applied to extract fluorescently stained regions, some partial deficiencies occur as shown Fig. 11, and they become a critical problem for the structural analysis of the neuron. Then our extraction method automatically interpolates these partial deficiencies.

In this paper, structural characteristics of the premotor neuron are extracted from the three-dimensional form which is extracted with our method.

3.2 Shape and structural characteristics of a premotor neuron based on knowledge of biologist

As previously indicated, Mishima and Kanzaki (1999) have identified three premotor neurons which are shown in Fig. 10 by visually discriminating structural configuration. In addition, the morphological characteristics of each premotor neuron were indicated, too. Based on these observations, biologists focus attention on following points in nerve fibers which extend to LAL and VPC ipsilateral to the soma when they identify these neurons.

[Key point 1] Characteristics of a main branch

The main branch of Type B and Type C extend to VPC ipsilateral to the soma. This makes main branch's length of these types is longer than Type A.

[Key point 2] Positional relation between a main branch and sub-branches which diverge from the main branch

Nerve fibers of Type A extend to the LAL. It means that

Table 3. Way which nerve fibers.

Type A	superiorly in whole
Type B	from right to left or up and down
Type C	down in whole

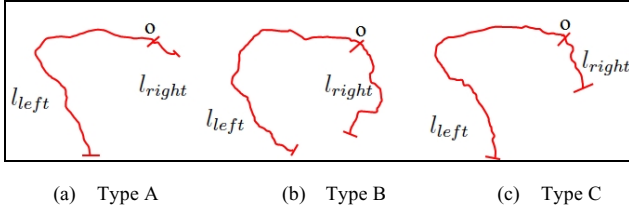


Fig. 13. Example of lengths of a main branch from origin to end points.

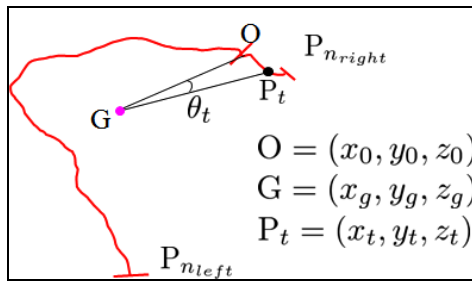


Fig. 14. Angle and length.

these nerve fibers extend from near points at the intersection of the main branch with the branch which is connected to the soma to the LAL. This intersection point is called an origin in this paper.

On other hand, nerve fibers of Type B extend to the LAL and VPC. Therefore these nerve fibers extend from anywhere. In Type C, because nerve fibers extend to the VPC, these nerve fibers extend from points which are at a side distant from the origin.

[Key point 3] Way which nerve fibers extend

Nerve fibers of each type tend to extend as Table 3.

In this paper, as shown Fig. 12, nerve fibers are separated the right and left as of an origin; nerve fibers that are in ipsilateral to the soma are branches of the right side, and branches on the side opposite to it are branches of the left side.

3.3 Extraction of structural features from three-dimensional form of neuron for comparison

We proposed quantities as features for structural comparison based on point of a biologist's observation as shown Table 2. These features are obtained from nerve fibers of the right side because structural characteristics based on empirical knowledge of biologists are shown in nerve fibers of right side. It is necessary to identify individual branches for calculation of features. Our extraction method of the neuron's form can identify individual branches easily. Because our method interpolates partial deficiencies every branch and each branch are connected at branching points (Saito and Toriwaki, 1993; Saito *et al.*, 1996) which are extracted from binarized CLSM images. Details of each feature are

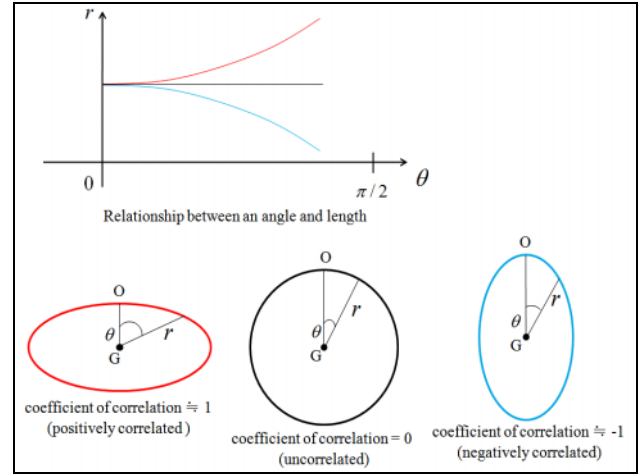


Fig. 15. Relationship between angle and length.

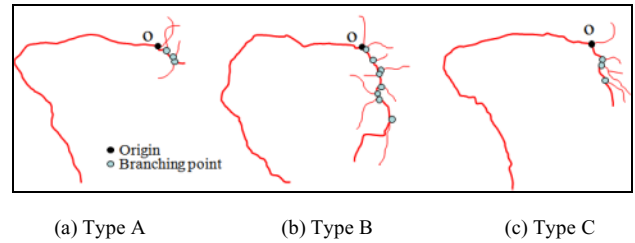


Fig. 16. Origin and branching point on the main branch.

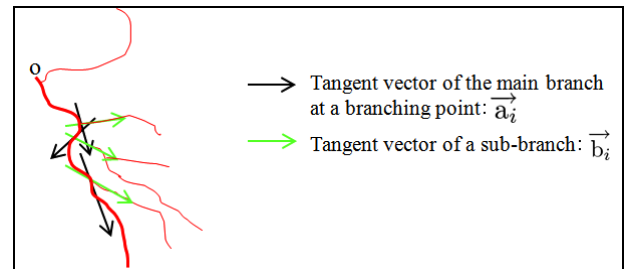


Fig. 17. Angles between the main branch and sub-branches.

described with a biologist's observation as follows.

[Feature 1]

There are characteristics in the length of a main branch (Key point 1). Then the ratio of lengths of the right side of a main branch to the whole length of main branch is set as Feature 1. This feature is obtained with Eq. (1). Each length is approximated with Simpson's rule. Figure 13 shows examples of length of a main branch from the origin to each end point.

$$f_1 = R_{\text{right}} = \frac{l_{\text{right}}}{l_{\text{left}} + l_{\text{right}}}. \quad (1)$$

[Feature 2]

In Type A, the main branch of right side extends in a different direction with other types (Key point 1). A main branch of right side in Type B and Type C extend in a downward direction. In contrast, Type A ones extend in crosswise direction. This characteristic is represented by appearance of curvature variation. Then an angle between

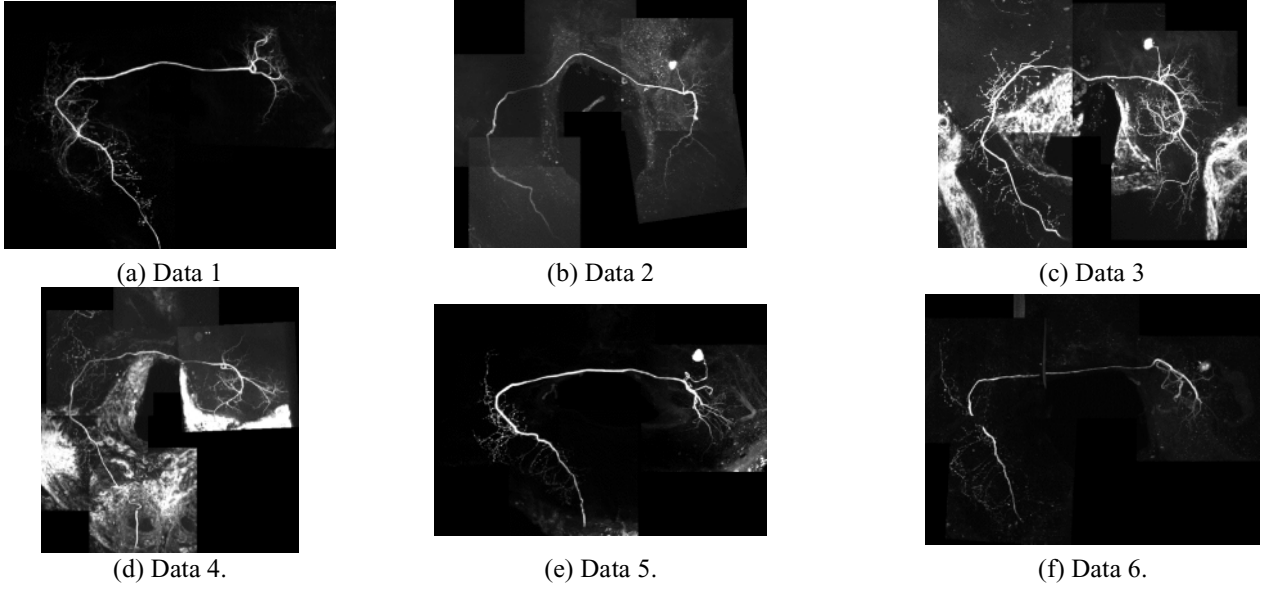


Fig. 18. CLSM cross-sectional image series of premotor neurons of silkworm moths (projection image).

a line passing from the median point of main branch to the origin and to a point which is on a main branch and length of these lines are calculated as indicated Fig. 14. In Fig. 14, O is the origin and G is the median point of main branch, and P_t is a point on a main branch, and t is $(0, 1, \dots, n_{\text{right}})$: n_{right} is number of voxel on the main branch of right side, and P_0 is the origin. Therein, median point is obtained by averaging out coordinate values of a main branch. A correlation coefficient of these angles and lengths is set as Feature 2. This correlation coefficient is obtained with Eqs. (2)–(6).

$$f_2 = r = \frac{\sum_{t=0}^{n_{\text{right}}} (\theta_t - \bar{\theta})(l_t - \bar{l})}{\sqrt{\sum_{t=0}^{n_{\text{right}}} (\theta_t - \bar{\theta})^2} \sqrt{\sum_{t=0}^{n_{\text{right}}} (l_t - \bar{l})^2}}. \quad (2)$$

Where

$$\theta_t = \cos^{-1} \left(\frac{\vec{GP}_t \cdot \vec{GO}}{|\vec{GP}_t| |\vec{GO}|} \right) \quad (3)$$

$$l_t = |\vec{GP}_t| = \sqrt{(x_g - x_t)^2 + (y_g - y_t)^2 + (z_g - z_t)^2} \quad (4)$$

$$\bar{\theta} = \frac{1}{n_{\text{right}}} \sum_t \theta_t \quad (5)$$

$$\bar{l} = \frac{1}{n_{\text{right}}} \sum_t l_t. \quad (6)$$

Figure 15 shows the relationship between the angle and length. It is possible to replace a shape of main branch with an oval sphere in which a median point is the origin. If a main branch extends in crosswise direction, the coefficient correlation nears 1 and this branch has been positively correlated. In addition, if a main branch extends in downward direction, the coefficient correlation nears -1 : negatively

correlated. This feature expresses a shape of main branch of right side.

[Feature 3]

Each type has the characteristics in location which nerve fibers extend to. In Type A, nerve fibers spread to the whole LAL. This means many branching points are in near the origin. In addition, in Type B, because nerve fibers extend to the LAL and the VPC, branching points can be anywhere (Fig. 16). By the same token, in Type C, branching points are removed from the origin because nerve fibers of Type C extend to the VPC. Therefore second-order moment and the mean coordinates of the branching points at the origin is set as Feature 3 in order to calculate relationship between the origin and branching points on the main branch. This feature is based on Key point 2 and obtained with Eqs. (7), (8), and (9); $E(l^2)$ and $E(l)$ are second-order moment and a mean distance from origin to a branching point, respectively, and m is the number of sub-branches. Distance from the origin to a branching point is the Euclidean distance obtained using Eq. (9).

$$f_{3-1} = E(l) = \frac{1}{m} \sum_{i=1}^m l_i \quad (7)$$

$$f_{3-2} = E(l^2) = \frac{1}{m} \sum_{i=1}^m l_i^2 \quad (8)$$

where

$$l_i = \sqrt{(x_i - x_0)^2 + (y_i - y_0)^2 + (z_i - z_0)^2}. \quad (9)$$

[Feature 4]

Biologists focus attention on whether nerve fibers spread in the LAL or not and how they spread. Then breadths of the distribution of the coordinate values which are the near origin are set as Feature 4. This means the difference of distribution of nerve fibers in the LAL. This feature is obtained with an eigenvalue of Eq. (10). Equation (10) indicates a variance-covariance matrix of coordinate values

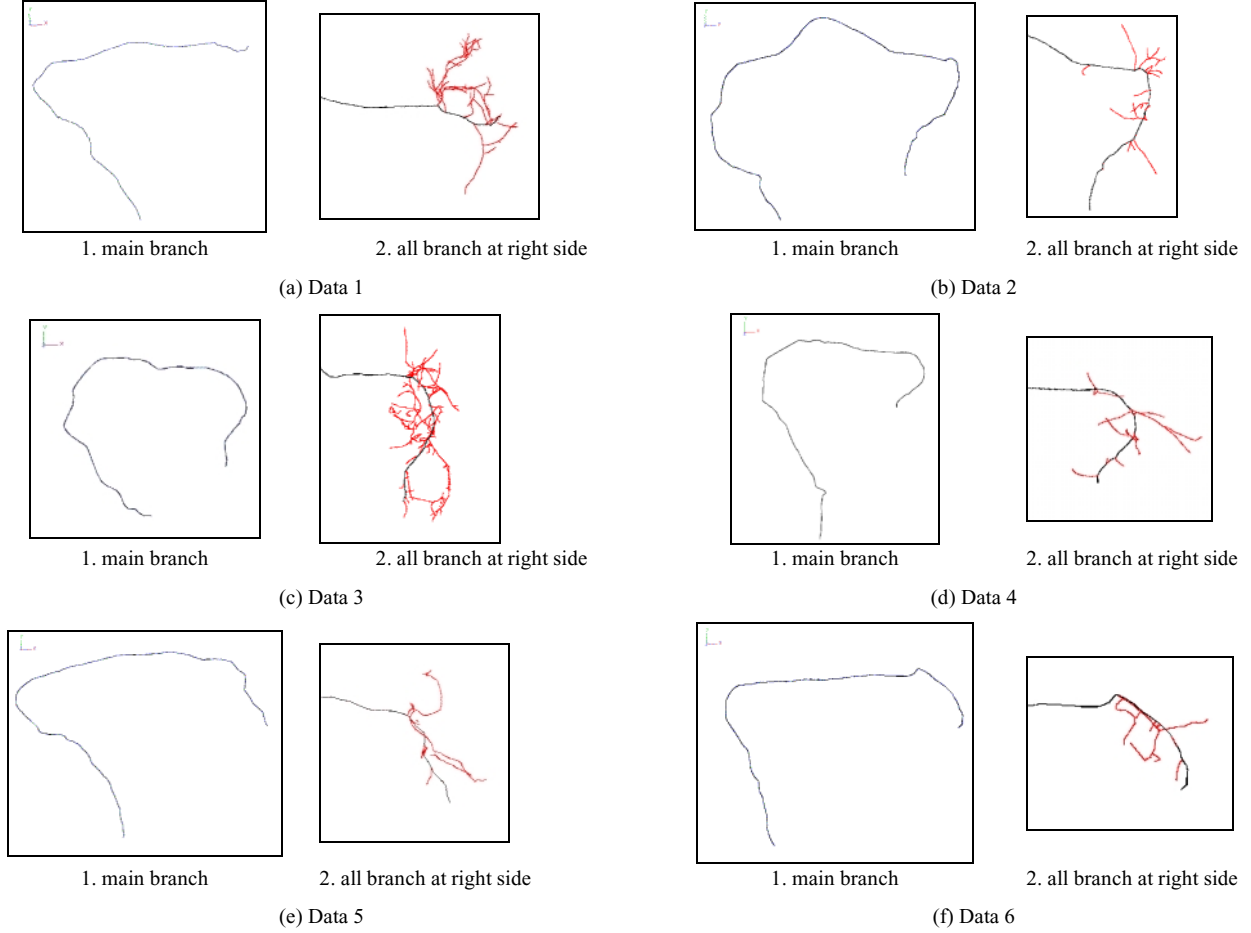


Fig. 19. Extraction result of form of premotor neurons using our interpolation method.

and Eqs. (12) and (13) mean covariance and average of x -coordinate and y -coordinate respectively. Therein n is the number of coordinates of nerve fibers. It is very difficult to identify the LAL region because the LAL region shows close similarity to the other surrounding regions. Then in this paper, LAL region is approximated by a region within d from origin; d is threshold of distance from origin and set empirically. Three eigenvalues are obtained from Eq. (10): λ_1 , and λ_2 , and λ_3 ($\lambda_1 \geq \lambda_2 \geq \lambda_3$). It is thought that λ_1 is the widest breadth of distribution and it means extensity of longitudinal direction. λ_2 represents a characteristics of Key point 2. Then λ_2 is set as Feature 4.

$$V = \begin{pmatrix} \sigma_{xx} & \sigma_{xy} & \sigma_{xz} \\ \sigma_{yx} & \sigma_{yy} & \sigma_{yz} \\ \sigma_{zx} & \sigma_{zy} & \sigma_{zz} \end{pmatrix}. \quad (10)$$

Where

$$\sigma_{xy} = \frac{1}{n} \sum_i (x_i - \bar{x})(y_i - \bar{y}) \quad (11)$$

$$\bar{x} = \frac{1}{n} \sum_i x_i \quad (12)$$

$$\bar{y} = \frac{1}{n} \sum_i y_i. \quad (13)$$

Table 4. Physiological response results and experimental data.

Physiological response	Data	Type
Flip-Flop	Data 1	Type A
Long-lasting inhibition	Data 2 and Data 3	Type B
	Data 4, Data 5, and Data 6	Type C

[Feature 5]

Nerve fibers of each type tend to extend in a characteristic manner, respectively (Key point 3). Then, an angle between the main branch and sub-branch is calculated with Eq. (15) as indicated in Fig. 17 in order to represent direction sub-branch extend. Therefore variation and mean of this angle are set as Feature 5. Feature 5 is obtained with Eqs. (14), (15), and (16).

$$f_{5-1} = \bar{\theta} = \frac{1}{m} \sum_{i=1}^m \theta_i. \quad (14)$$

Where

$$\theta_i = \cos^{-1} \left(\frac{\vec{a}_i \cdot \vec{b}_i}{\|\vec{a}_i\| \|\vec{b}_i\|} \right) \quad (15)$$

$$f_{5-2} = v_\theta = \frac{1}{m} \sum_{i=1}^m (\theta_i - \bar{\theta})^2. \quad (16)$$

Table 5. Extraction results of features from three-dimensional form.

Data	Feature 1	Feature 2	Feature 3		Feature 4	Feature 5	
			1. Average	2. Variance		1. Average	2. Variance
1	0.07	0.88	24.56	926.47	6270.00	1.35	0.27
2	0.26	-0.86	49.35	3835.76	101.20	1.63	0.37
3	0.26	-0.84	48.62	4238.26	812.71	1.29	0.51
4	0.15	-0.81	40.54	2151.77	0	1.37	1.09
5	0.15	0.93	23.87	834.82	0	1.61	0.31
6	0.17	0.99	38.96	1973.19	0	1.47	0.19

Results of features extraction are shown Table 5, and these results are graphed in Fig. 20.

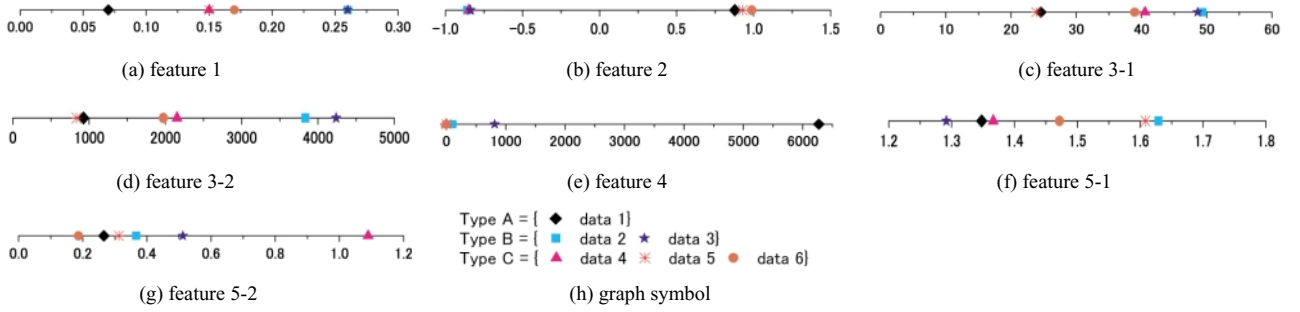


Fig. 20. Extraction results of features.

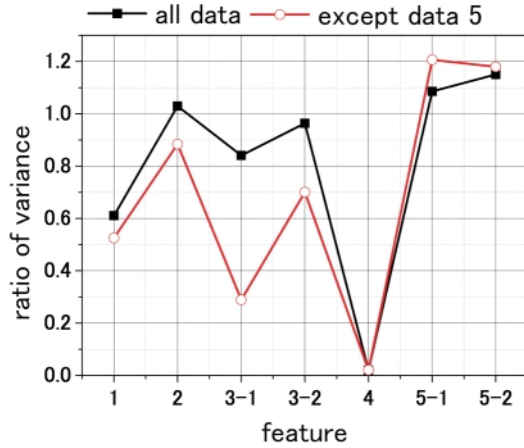


Fig. 21. Ratio of variation of data which is except data 1 to variance of all data (the red line is about all data except data 5) in each feature.

Each feature is categorized as feature which means shape or structure as like Eqs. (17) and (18).

$$F_{\text{form}} = \{f_1, f_2\} \quad (17)$$

$$F_{\text{structure}} = \{f_3, f_4, f_5\}. \quad (18)$$

In this paper, premotor neurons are comparing objectively using these features.

4. Experimental Results

The proposed method was applied to the cross sectional image series of premotor neurons as shown in Fig. 18. Figure 18 is obtained using CLSM. Figure 19 shows extraction results of main branch and all branches of right side

Table 6. Categorized result with each feature.

Feature	Same category as result using physiological response characteristics
1	NO
2	NO
3-1	YES (except data 5)
3-2	NO
4	YES
5-1	NO
5-2	NO

using our interpolation method. Proposed features are obtained with the main branch and sub-branches which are on the main branch. Then in this experiment, we targeted the main branch and sub-branch; these branches make principal form of premotor neuron. All figures in Fig. 19 are visualized three-dimensionally using V-Cat which is software for three-dimensional visualization (RIKEN, 2004).

Proposed features are extracted from these three-dimensional form images. In Feature 5, threshold for identify of the LAL region is 80 which is Euclidean distance from origin. In this experiment, proposed features are estimated by classifying data into the category which is same with using physiological response result. Table 4 shows physiological response results of each data, and types in Table 4 are categorized based on (Mishima and Kanzaki, 1999).

Biologists focus attention on feature of shape in visual comparison. Hence, in Fig. 19, comparison results using Feature 2 which expresses shape are categorized {Type B}

and {Type A and Type C}. However, Feature 1 is also set as feature which express shape, comparison results are categorized {Type A}, {Type B}, and {Type C}. This means visual comparison is very ambiguous; there is difference between neurons by quantizing characteristics of shape if shape is similar in visually. Comparison results using Feature 3-1 (except data 5) and Feature 4 indicated structure of Type B and Type C is similar.

In addition, Fig. 21 shows ratios of variation of all data other than data 1 to variance of all data in each feature (Eq. (19)).

$$R_{\text{variance}} = \frac{\text{variance of all data other than data 1}}{\text{variance of all data}}. \quad (19)$$

In Fig. 21, a red line is ratios of variation of all data other than data 1 to variance of all data other than data 5. If this ratio is small, variance of data except data 1 is small. This means distance between data 1 and other data is great in this feature; it is easy to classify data into data 1 and other data.

These results show it is not necessary that a neuron which is similar in shape have the same structure. Table 4 shows whether each data can be classified with this feature under the same category as classified results with physiological response characteristics. With this result and Fig. 20, it is found that Feature 4 and Feature 3-1 express structures of premotor neurons. In other word, these features are strongly associated with function of premotor neuron.

In addition, ratios of variation in Feature 4 and Feature 3-1 (except data 5) are under 0.4 and these results are estimated quantitatively. In addition, it becomes clear that Type B has no considerable individual variability in data 2 and data 3. On other hand, Type C has some. These results show objective comparison of premotor neurons is possible. For more detail elucidation, it is needed to apply our proposed method to more data in order to become structural similarity and dissimilarity between neurons more appear.

5. Conclusion

We presented a method for objective comparison of shape and structure of premotor neurons in silkworm moth brain. Difference of shape and structure of premotor neuron is unknown in detail because there is no way of analysis of structure apart from visual inspection. Then we proposed a method of comparing neuronal shape and structures using image processing techniques. The proposed method extracted seven features which are based on biologist's empirical knowledge from three-dimensional form of a premotor neuron.

As a result, features which indicator neuronal structures are found by estimating using physiological response characteristics. In other words, it is found that these features are strongly associated with neuronal function. In addition, differences in structure and shape between three premotor neurons are found. These mean ambiguous evaluation criteria of biologists are quantified. These results lead to the suggestion that it is not necessary that neurons which have the same shape have the same structure and that there is no relationship between neuronal shape and function. Consequently, it is found that using not neuronal shape but struc-

ture for elucidation of neuronal function is important; a neuronal function is presumable by analyzing neuronal structures.

In addition, structural similarity and dissimilarity between neurons are suggested in this paper. It becomes to be possible that a standard model of neuron is constructed by extracting structural features from more neuronal form data and by discussion about more suitable feature. Moreover, elucidation of information propagation mechanisms by simulation with this model is archived.

Acknowledgments. This work was partially supported by a Grant-in-Aid for Scientific Research on Priority Areas "Emergence of Adaptive Motor Function through Interaction between Body, Brain and Environment" from the Japanese Ministry of Education, Culture, Sports, Science and Technology.

References

- Evers, J. F., Muench, D. and Duch, C. (2006) Developmental relocation of presynaptic terminals along distinct types of dendritic filopodia, *Developmental Biology*, **297**, 214–227.
- Ikeno, H. (2004) Flight control of honeybee in the y-maze, *Neuroncomputing*, **58–60**, 663–668.
- Jaap, V. P., Arjen, V. O. and Harry, B. U. (2001) The need for integrating neuronal morphology database and computational environments in exploring neuronal structure and function, *Anatomy and Embryology*, **204**, No. 4, 255–265.
- Kanzaki, R., Sugi, N. and Shibuya, T. (1992) Self-generated zigzag turning of *Bombyx mori* males during pheromone-mediated upwind walking, *Zoological Science*, **9**, 515–527.
- Kanzaki, R., Ikeda, A. and Shibuya, T. (1994) Morphological and physiological properties of pheromone-triggered flipflopping descending interneurons of the male silkworm moth, *Bombyx mori*, *Journal of Comparative Physiology A*, **175**, 1–14.
- Karl, V. F. (1974) Decoding the language of the bee, *Science Magazine*, **185**, No. 4152, 663–668.
- Kawabata, K., Fujiki, T., Ikemoto, Y., Aonuma, H. and Asama, H. (2007) A neuromodulation model for adaptive behavior selection by the cricket, *J. Robotics and Mechatronics*, **19**, No. 4, 388–394.
- Mishima, T. and Kanzaki, R. (1999) Physiological and morphological characterization of olfactory descending interneurons of the male silkworm moth, *Bombyx mori*, *Journal of Comparative Physiology A: Neuroethology, Sensory, Neural, and Behavioral Physiology*, **184**, No. 2, 143–160.
- Nakajima, K., Morishita, S., Kazawa, T., Kanzaki, R., Kawabata, K., Asama, H. and Mishima, T. (2009) Interpolation of binarized CLSM images for extraction of premotor neuron branch structures in silkworm moth, *Sensor Review*, **29**, 137–147.
- Nishikawa, I., Nakamura, M., Igarashi, Y., Kazawa, T., Ikeno, H. and Kanzaki, R. (2008) Neural network model of the lateral accessory lobe and ventral protocerebrum of *Bombyx mori* to generate the flip-flop activity, in *Seventeenth Annual Computational Neuroscience Meeting*, 23.
- Ridgel, A. L., Blythe, E. A. and Roy, E. R. (2007) Descending control of turning behavior in the cockroach, *Blaberus discoidalis*, *Journal of Comparative Physiology A: Neuroethology, Sensory, Neural, and Behavioral Physiology*, **193**, No. 4, 385–402.
- RIKEN (2004) V-Cat, available at: http://vcad-hpsv.riken.jp/en/release_software/V-Cat/ (accessed 2 June 2008).
- Saito, T. and Toriwaki, J. (1993) Reverse euclidean distance transformation and extraction of skeletons in the digital plane, *IEICE Technical Report, Pattern Recognition and Understanding*, **93**, No. 228, 57–64.
- Saito, T., Mori, K. and Toriwaki, J. (1996) A sequential thinning algorithm for three dimensional digital pictures using the euclidean distance transformation and its properties, *The Transactions of IEICE*, **J79-D-2**, No. 10, 1675–1685.
- Sandeep, R. D., Maria, L. V., Vanessa, R., Sean, L., Allan, W., Ebru, D., Jorge, F., Karen, B., Barry, J. D. and Richard, A. (2008) The drosophila pheromone cva activates a sexually dimorphic neural circuit, *Nature (London)*, **452**, 473.
- Seki, Y., Aonuma, H. and Kanzaki, R. (2005) Pheromone processing center in the protocerebrum of *Bombyx mori* revealed by nitric oxide-induced

- anti-cGMP immunocytochemistry, *The Journal of Comparative Neurology*, **480**, 340–351.
- Urata, H., Isokawa, T., Seki, Y., Kamiura, N., Matsui, N., Ikeno, H. and Kanzaki, R. (2007) Three-dimensional classification of insect neurons using self-organizing maps, *Lecture Notes in Computer Science*, **4694**, 123–130.
- Wada, S. and Kanzaki, R. (2005) Neural control mechanisms of the pheromone-triggered programmed behavior in male silkworms revealed by double-labeling of descending interneurons and a motor neuron, *The Journal of Comparative Neurology*, **484**, 168–182.
- Yamanaka, N., Hua, Y., Mizoguchi, A., Watanabe, K., Niwa, R., Tanaka, Y. and Kataoka, H. (2005) Identification of a novel prothoracicostatic hormone and its receptor in the silkworm *Bombyx mori*, *The Journal of Biological Chemistry*, **280**, No. 15, 14684–14690.